Available online at www.sciencedirect.com
SCIENCE DIRECT®

Journal of the European Ceramic Society 24 (2004) 3251–3259

www.elsevier.com/locate/jeurceramsoc

Preparation of porous SiC ceramic with a woodlike microstructure by sol-gel and carbothermal reduction processing

Jun-Min Qian*, Ji-Ping Wang, Guan-Jun Qiao, Zhi-Hao Jin

State Key Laboratory for Mechanical Behavior of Materials, School of Materials Science and Engineering, Xi'an Jiaotong University, Xi'an 710049, People's Republic of China

Received 20 August 2003; received in revised form 14 October 2003; accepted 25 October 2003

Abstract

Highly porous silicon carbide ceramic with a woodlike microstructure has been prepared by carbothermal reduction reaction of charcoal/silica composites in static argon atmosphere, which were fabricated by infiltrating silica sol into a porous biocarbon template from tilia amurensis wood using a vacuum/pressure infiltration process. The morphology of resulting porous SiC ceramic, as well as the conversion mechanism of wood to porous SiC ceramic, have been investigated by scanning electron microscopy (SEM), X-ray diffraction (XRD), Fourier transform infrared spectroscopy (FTIR), and thermogravimetric analysis (TGA) and differential scanning calorimetry (DSC) techniques. Experimental results show that the biomorphic cellular morphology of tilia amurensis wood charcoal tissue is remained in the porous SiC ceramic with high precision which consists of β-SiC with traces of α-SiC. The strut thickness of resulting SiC ceramic becomes thinner, even partially disappears with the increase of silica amount contained in the charcoal/silica composites. The morphology of the SiC ceramic reveals that solid–solid, gas–solid and gas–gas reactions occurred during the charcoal-to-ceramic conversion.

Keywords: Biomorphic SiC; Carbothermal reduction; Microstructure; Porous ceramics; SiC; Sol-gel processes; Wood

1. Introduction

Design of novel ceramic materials with specific functional properties and structures by mimicking the hierarchical cellular structure of wood has recently attained particular interest[1–3] owing to a remarkable combination of good mechanical property at low density, corrosion resistance, overcoming the environmental and economical issues caused by traditional manufacturing, and a unique microstructure pseudomorphous to wood.[4] Wood is a naturally grown composite material of complex hierarchical cellular structure, and comprised of elongated tubular cells aligned with the axis of the tree trunk and growth ring structures which are the reason for the macroscopic inhomogeneity of natural wood.[5] The tubular cells of wood with a preferential orientation in axial direction offer the possibility to use various infiltration techniques to transform the bioorganic wood structure into an inorganic ceramic material with tailored physical and mechanical properties, and may serve as a hierarchical template to generate novel cellular ceramics with a micro-, meso- and macro-structures pseudomorphous to the initial porous tissue skeleton spanning in typical dimensions ranging from nanometers (cell wall fibrils) to millimeters (growth ring patterns).[2,6]

Wood-derived cellular ceramics with homogeneous (monomodal) or heterogenous (multimodal or fractal) anisotropic pore structures might be of interest for high-temperature-resistant exhaust gas filters, catalyst carriers in energy and environmental technology, advanced microreactor systems, bioinert and corrosion resistant multifunctional immobilization supports for living cells, microbes or enzymes in food industry, medicine and biotechnology, and waste water treatment, as well as acoustic and heat insulation structures, etc.

Wood has been used to prepare woodceramics, woodceramics/metal composites, porous SiC or TiC ceramics, porous oxide ceramic, and biomorphic Si/SiC composites.[3,7–12] Previous work on converting wood

* Corresponding author. Tel.: +86-29-2667942; fax: +86-29-2665443.
E-mail address: junminqian@hotmail.com (J.-M. Qian).

0955-2219/$ - see front matter © 2003 Elsevier Ltd. All rights reserved.
doi:10.1016/j.jeurceramsoc.2003.10.042

into various SiC ceramic materials focused on the infiltration of the pyrolysed biocarbon template with gaseous or liquid silicon bearing precursors such as silicon melt, silicon and silicon monoxide vapor, and organosilicon compounds at high temperatures,[2,13–16] and silica sol from tetraethylorthosilicate (TEOS) at low temperature followed by pryolysis in inert atmosphere.[17] In terms of economy and efficiency, sol-gel mothod is the best choice. It involves inexpensive silicon dioxide and carbon (or carbon precursors) as the starting materials.

Sol-gel technology has been utilized to prepare ceramic materials using reactive replica techniques,[18] owing to low cost, no troublesome procedure, and allowing lower temperatures of synthesis. SiC materials previously produced by sol-gel methods mainly focus on SiC powders, fibers, and whiskers.[19–24] Recently, some advanced SiC materials such as nanowires, nanorods and nanometer-sized powders or whiskers, have been prepared by sol-gel methods.[25] For example, fine SiC tubes were prepared by sintering and gasifying carbon fibres covered with a silica layer produced by a sol-gel method.[26,27] Mesoporous SiC powders were produced from TEOS and phenolic resin with nickel nitrate as a pore-adjusting reagent by a modified sol-gel method.[28] It appears that in a more general way, SiC materials of desired design may be prepared by an appropriate selection of the silica–carbon artefact. Moreover, it would be also of great interest to control the texture of the produced material.

In the present study, we attempt (i) to demonstrate the possibility of producing porous SiC ceramic with a woodlike microstructure starting from silica infiltrated tilia amurensis charcoal and (ii) to investigate the carbothermal conversion of the charcoal–silica composites into SiC by heat treatment in argon atmosphere using SEM, XRD, TGA and FTIR techniques.

2. Experimental

2.1. Material preparation

Tilia amurensis wood was shaped, dried at 110 °C for 2–4 days, and subsequently carbonized under vacuum at 1200 °C for 4 h in a graphite heater furnace with a slow heating rate of 2 °C/min up to 600 °C and a higher rate of 5 °C/min up to the peak temperature, resulting in a porous biocarbon template (charcoal). Silica sol was prepared from ethanol solutions of tetraethoxysilane [$Si(OC_2H_5)_4$, TEOS], distilled water and hydrochloric acid at a suitable molar ratio of TEOS:H_2O:HCl by a sol-gel process as that described elsewhere.[26,29] In the present work, the concentration of silica sol was equal to 20% by weight.

Charcoal was placed in an infiltration vessel in a self-made equipment. The vessel was evacuated and held for 3 h, and then backfilled with silica sol. After that, the pressure in the vessel was raised to a high atmosphere pressure of 1.5 MPa with 6 h hold. The silica sol contained in charcoal was gelled at 60 °C for 20 h and dried at 120 °C for 8 h to remove other solvents, resulting in silica–charcoal composites. The treatment procedure of impregnation, gelling and drying, namely cycle of impregnation procedure, was repeated several times, to increase the silica content in charcoal–silica composites.

Carbothermal reduction of the as-prepared silica–charcoal composites was carried out in static argon atmosphere in a graphite heater furnace at 1600 °C with a rate of 600 °C/h to form porous SiC ceramic. The reactant silica–charcoal composites loaded in graphite crucibles were placed into the hot zone of the furnace. The temperature of the furnace was raised up to the desired temperature, and then held for 4 h to allow complete reaction of silica with the carbon structure to form β-SiC. Fig. 1 summarizes the processing scheme.

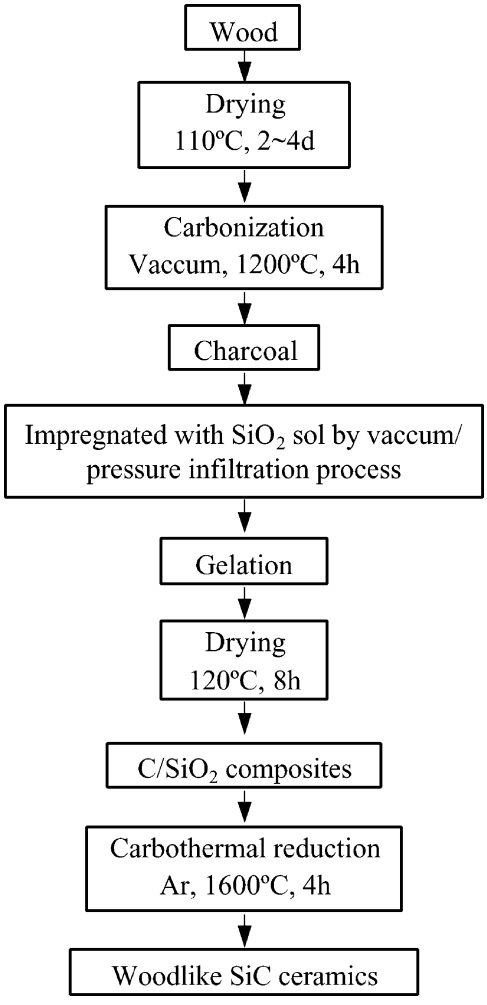

Fig. 1. Processing scheme of manufacturing woodlike SiC ceramic from tilia amurensis wood.

2.2. Characterization

The pyrolytic behavior of tilia amurensis wood was characterized using thermogravimetric analysis (TGA) and differential scanning calorimetry (DSC) in a N_2 flow-rate of 100 ml/min with a heating rate of 10 °C/min from room temperature to 900 °C. TGA and DSC were performed on DSC-TGA (model Netzsch Thermische Analyzer STA 409C) thermal analyzer with alumina powder as the reference sample.

The morphological changes of the starting material during the transformation of the charcoal/silica material into SiC ceramic were observed and analyzed by scanning electron microscopy (SEM, Hitachi, S-2700) operated at 20 kV and 20 mA. X-ray diffraction (XRD) was measured on a D/MAX-RA X-ray diffractometer to determine the crystalline phases formed during the carbothermal reduction reaction, using nickel filtered Cu $K\alpha$ radiation produced at 35 kV and 20 mA. The samples were pasted on a stub and then metallized with gold. Fourier transform infrared spectroscopy (FTIR) studies were performed with a Fourier transform infrared spectrometer (AVATAR 360 FT-IR, Nicolet) in the wavenumber range of 4000–500 cm^{-1}. The samples' spectra were recorded by transmission in dry air atmosphere through a pastille made of a few milligrams of sample materials mixed with KBr.

3. Results and discussion

3.1. Pyrolytic conversion of wood to carbon template

Wood may be converted by controlled thermal decomposition into a monolithic carbon template that retains the anatomical features of wood. In order to study the decomposition behavior of wood, some small pieces were heated in the thermal analyzer in N_2 atmosphere. Fig. 2 shows the TGA and DSC curves of tilia amurensis wood up to 900 °C. It can be seen that weight loss during heating of dried wood starts below 100 °C, reaches a maximum rate at 360 °C and is almost terminated at 500 °C. Although the TGA curve for tilia amurensis wood is quite similar in its nature to that of maple wood, the DSC curve shows slight differences due to differences in the chemical contents of tilia amurensis and maple woods.[4]

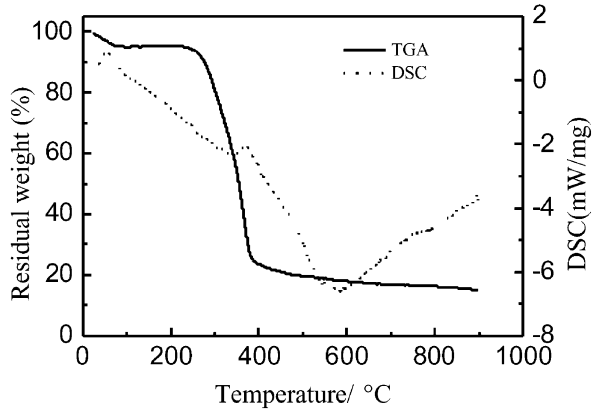

Fig. 2. TGA–DSC curves of tilia amurensis wood.

Mechanisms[30] involved in conversion of wood to carbon are: (a) desorption of adsorbed water up to 150 °C, (b) splitting of wood structure water between 150 °C and 260 °C, (c) chain scissions, or depolymerization, and breaking of C–O and C–C bonds within ring units evolving water, CO and CO_2 between 260 °C and 400 °C, (d) aromatization forming graphitic layers above 400 °C, and (e) above 800 °C, thermal induced decomposition and rearrangement reactions are almost terminated leaving a carbon template structure. The three major components of wood, namely hemicellulose, cellulose and lignin, break down in a stepwise manner at 200–280 °C, 260–350 °C and 280–500 °C, respectively.[31,32] Between 260 °C and 400 °C almost 80% of the total weight loss occurs which may vary between 40% (lignin) to about 80% (cellulose) due to evolution of H_2O, CO_2, and volatile hydrocarbon species from fragmentation reactions of the polyaromatic constituents via the open pore channel system of wood. The carbon template was shown to be easily machined to net shape prior to conversion to a ceramic material.[32]

3.2. XRD analysis

The XRD patterns of charcoal, silica/charcoal composite, and resulting porous SiC ceramics obtained after different number of cycles of impregnation procedure are shown in Fig. 3. It can be seen that two broad peaks centered around 22° and 44° in Fig. 3a, b suggest that both charcoal and charcoal/silica composite are amorphous. Peaks due to β-SiC (cubic type) phases are observed together with the broad peaks due to charcoal after one cycle of impregnation procedure (Fig. 3c), indicating that the formation of β-SiC has taken place and that residual free carbon still exists. The intensity of peaks due to β-SiC phases in the XRD patterns increases significantly with increasing the number of cycles of impregnation procedure, whereas the intensity of peaks (0002) and (0004) due to residual free carbon decreases (Fig. 3d), even disappears (Fig. 3e). In addition, one additional line at $2\theta = 33.82°$ ($d = 0.265$ nm) in the XRD patterns of porous SiC ceramics is detected near the (111) line of the cubic structure of the silicon carbide at $2\theta = 35.64°$ ($d_{111} = 0.251$ nm) which is characteristic of hexagonal polytypes (α-SiC phase).[33] Diffraction peak ($d_{101} = 0.404$ nm) for crystalline SiO_2 (cristobalite) is never observed, which indicates that nearly the whole amount of silica has been consumed during carbothermal reduction reaction. The results show that the

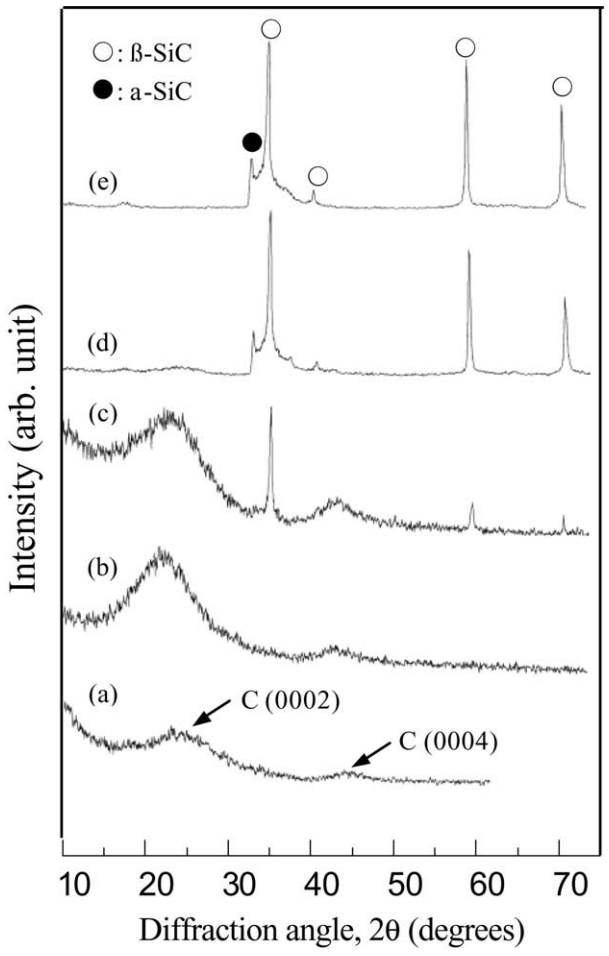

Fig. 3. Powder XRD patterns of (a) charcoal, (b) charcoal–silica composite and resulting woodlike SiC ceramics obtained at 1600 °C for 4 h when number of cycles of impregnation procedure is (c) 1, (d) 3 and (e) 5, respectively.

resulting porous products are essentially constituted of SiC of cubic type (β-SiC) with a minor amount of α-SiC. This would suggest that the C-SiC composites with various carbon contents can also be produced by selecting the C/Si ratio of the precursor silica/charcoal composites on the basis of this procedure. The optimum impregnation time is found to be 5, i.e., $C/SiO_2 \approx 3$ (Fig. 6), when very well crystallized β-SiC and a negligible residue of unreacted reactants are produced.

3.3. FTIR analysis

Fig. 4 shows the FT-IR spectra of charcoal/silica composite and porous SiC ceramic prepared from charcoal/silica composite after five cycles of impregnation procedure. In the IR spectrum (Fig. 4a) of the charcoal/silica composites, the absorption bands at 1090, 800 and 466 cm^{-1} are attributed to antisymmetric and symmetric stretching vibrations of Si–O–Si bond, respectively. Compared with the spectrum in Fig. 4a, the above-mentioned absorption bands nearly disappear

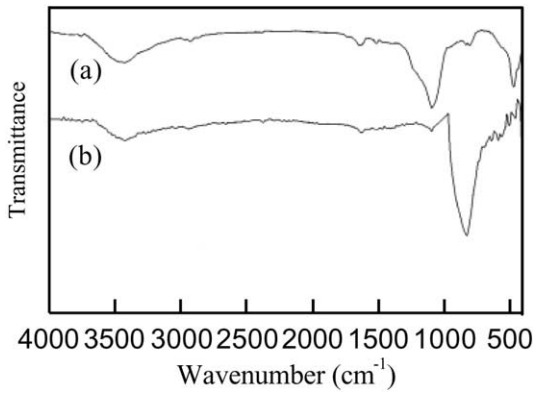

Fig. 4. Infrared spectra of (a) charcoal–silica composite and (b) porous SiC ceramic obtained by sintering charcoal–silica composite at 1600 °C for 4 h after five cycles of impregnation procedure.

in Fig. 4b. At the same time, a new intense broad band centred at 825 cm^{-1} is observed, which is ascribed to the Si-C fundamental stretching vibration,[29,34] in spite of some discrepancy between the wavenumber values indicated in the literature. In the case of pure SiC, an intense IR-absorption band at 840 cm^{-1} with a shoulder at 950 cm^{-1} has been found. For a SiC material prepared from a carbon/silica hydrogels, the broad band is located between 825 and 898 cm^{-1} (centered at 850 cm^{-1}). For some other authors,[35] the main band is located between 789 and 794 cm^{-1}. The discrepancy between the values is attributed to the different morphology of the analysed SiC. In addition, the low intensity broad band located between 1250 and 1000 cm^{-1} is assigned to the presence of a small fraction of silica that is negligible at the XRD sensitivity. This would imply that silica hardly remains in the porous SiC ceramic.

3.4. SEM analysis

Fig. 5 shows the cellular microstructures of biocarbon template from tilia amurensis wood. As seen in Fig. 5, the microstructure of the as-prepared tilia amurensis wood charcoal shows hollow channels of various diameters that originate from tracheid cells that are parallel to the axis of the tree. The channels can be classified into two groups, depending on their cross-sectional area (as shown in Fig. 5b): large channels (noted by "A") and small channels (noted by "B") that are in the vicinity of the larger channels and form a honeycomb structure. The average diameter of each group of cells is 50 μm for the large cells and 10 μm for the small cells, respectively. Most of the cellular pores show a round or elliptical shape. The cell topologically uniform arrangement of early wood is interrupted by growth ring patterns, where late wood cells show a significantly higher strut thickness.

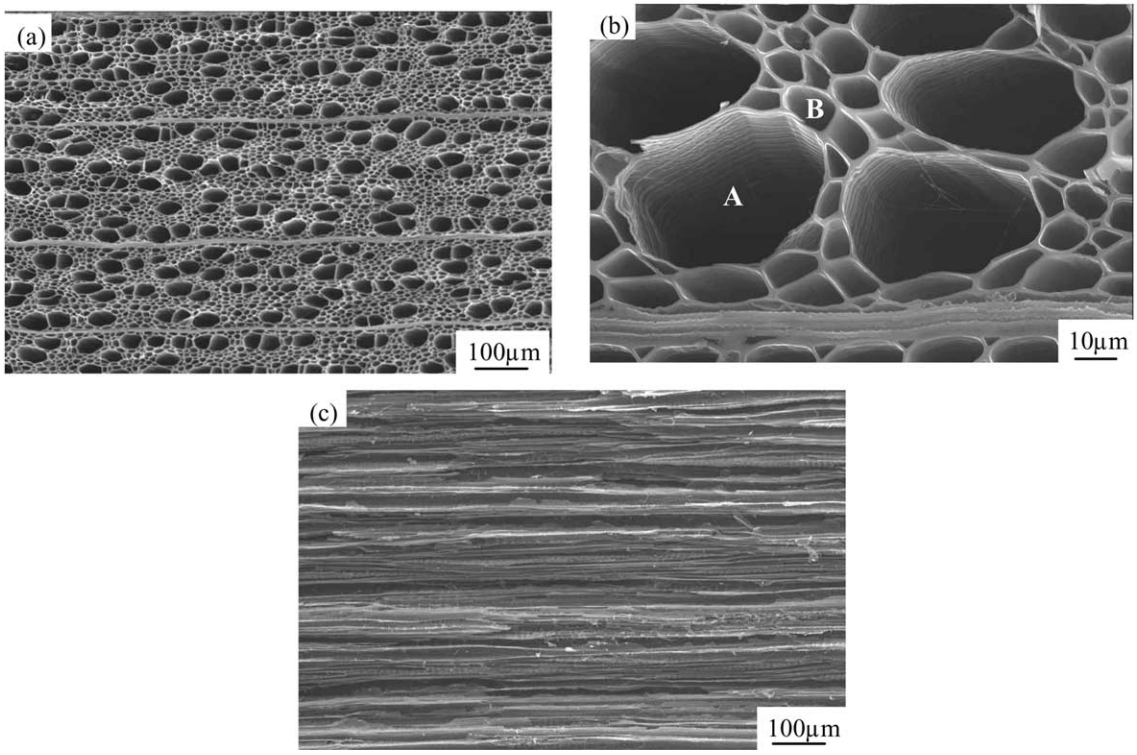

Fig. 5. SEM micrographs of carbonized tilia amurensis wood obtained at 1200 °C for 4 h: (a)–(b) cross sections perpendicular to axial direction, (c) cross section parallel to axial direction.

Silica content in charcoal–silica composite may be controlled by the number of cycles of impregnation procedure. Silica amount in the charcoal–silica composite increases as the number of cycles of impregnation procedure increases, as shown in Fig. 6. Silica amount quickly increases prior to the fifth treatment, tardily increases owing to "bottle-neck" effect of the cellular pores, and subsequently nearly becomes constant after the impregnation procedure with silica sol is repeated seven times. The SEM micrographs of the charcoal–silica composites are shown in Fig. 7. It is seen that fine SiO_2 gel fibers or rods appear in the cellular pores after impregnation procedure is repeated one time (Fig. 7a). The cellular pores are completely and uniformly filled up with dried SiO_2 gel when the impregnation procedure is repeated nine times (Fig. 7b).

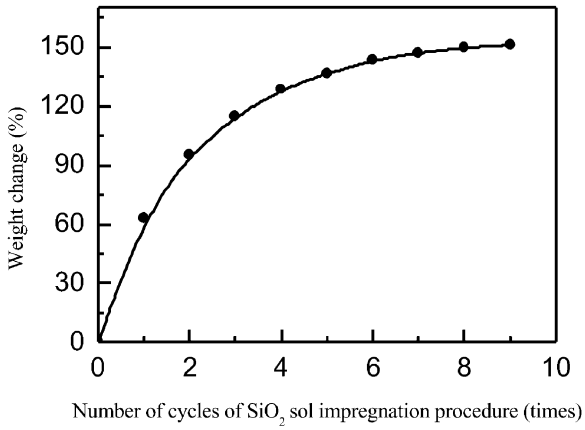

Fig. 6. Weight changes of SiO_2 contained in charcoal, relative to the increasing number of cycles of impregnation procedure.

The SEM micrographs of the resulting porous SiC ceramic are shown in Fig. 8. It can be seen that the resulting SiC material is of a microstructure pseudomorphous to biocarbon template derived from tilia amurensis wood. The struts are composed of SiC particles with typical diameter of about 2 μm, and some nanometer needle-like SiC whiskers with lengths of up to 10 μm can be observed in few cellular pores. The thickness and density of the struts of the products are decided by silica content in charcoal/silica composite that depends on the number of cycles of impregnation procedure. The thickness of the struts becomes thinner, and density becomes smaller with the increase in number of cycles of impregnation procedure (Fig. 9). From SEM observations it is concluded that the SiC forming the cell wall material between the cells is highly porous in the initial state of reaction, making rapid gas transport possible. In the literature,[36,37] half of the initial carbon is supposed to be released from the template via CO(g) [produced by reaction (5)] evaporation leaving a substationally higher porosity in the cell wall. Thus, tailoring of the strut microstructure by suitable processing techniques seems to play a key role for improving the mechanical properties of low-density biomorphous silicon carbide ceramics. It is reported that increasing

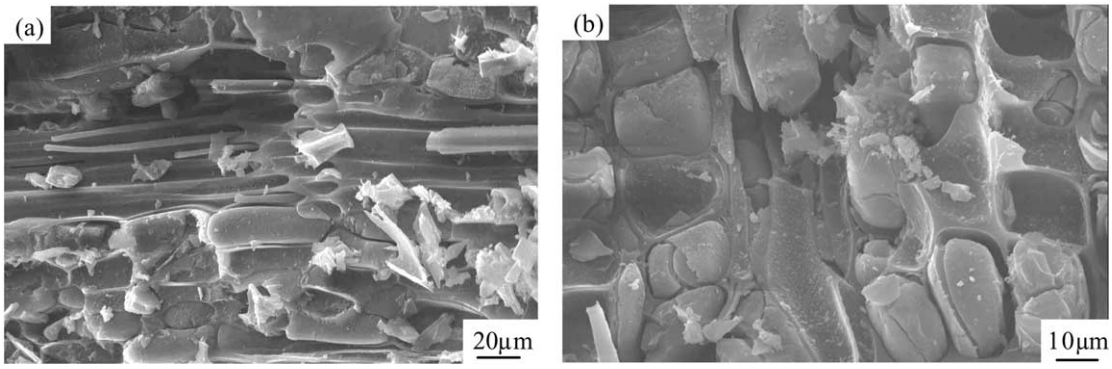

Fig. 7. SEM micrographs of charcoal–silica composites when the impregnation procedure is repeated (a) 1 and (b) 9 times, respectively.

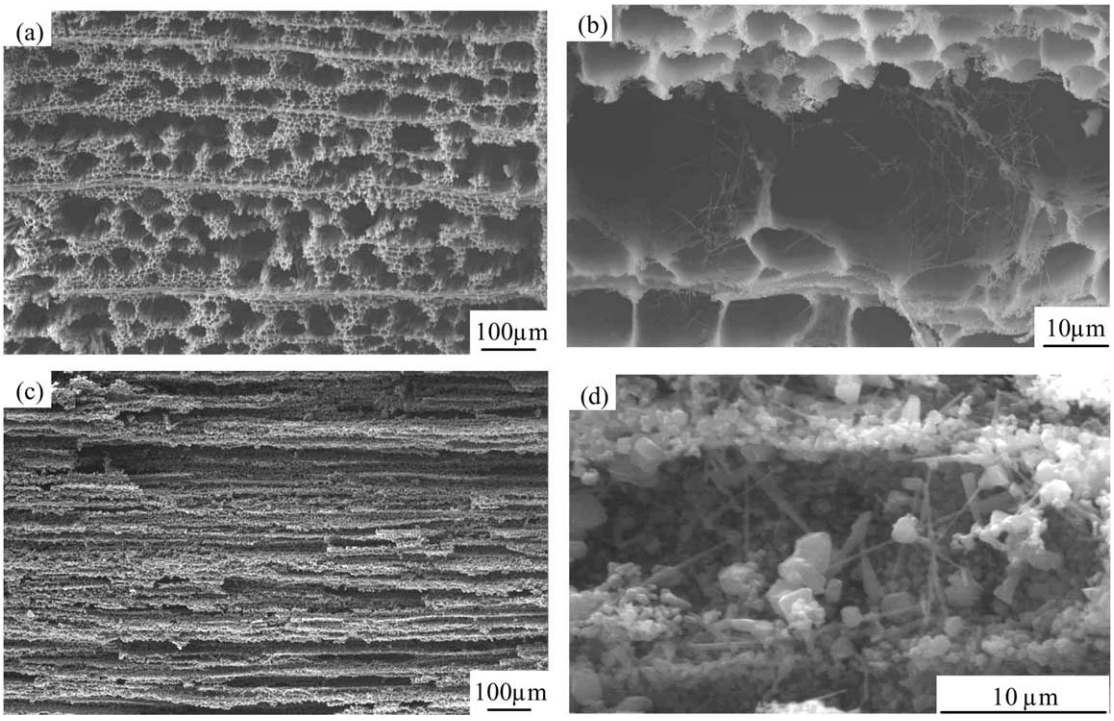

Fig. 8. SEM micrographs of woodlike β-SiC ceramic manufactured by sol-gel and carbothermal reduction processing at 1600 °C for 4 h when impregnation procedure is repeated twice: (a)–(b) cross sections perpendicular to axial direction and (c)–(d) cross sections parallel to axial direction. (a) and (c) are low-magnification SEM images. (b) and (d) are high-magnification SEM images.

the strut thickness and density may result in an improvement of mechanical strength of highly porous material by selecting original wood.[38]

3.5. Mechanism of conversion of charcoal/silica composite into SiC ceramic

It has been shown[26] that under the experimental conditions of the present work, the overall reaction between charcoal and silica for producing silicon carbide is:

$$SiO_2(s,l) + 3C(s) \rightarrow SiC(s) + 2CO(g) \quad (1)$$

In fact, reaction (1) proceeds through two stages in which a gaseous intermediate, silicon monoxide (SiO) gas is formed. The first step consists of a solid-solid or solid-liquid type of reaction between carbon and silica leading to the formation of gaseous silicon monoxide (SiO) and carbon monoxide (CO) according to reaction (2)

$$SiO_2(s,l) + C(s) \rightarrow SiO(g) + CO(g) \quad (2)$$

where s, l and g refer to the solid state, the liquid state and the gas state, respectively. Eq. (2) is either a purely solid–solid or a liquid–solid reaction (above 1450 °C, quartz melts).[20] Once carbon monoxide (CO) is formed, SiO can also be produced according to reaction

$$SiO_2(s) + CO(g) \rightarrow SiO(g) + CO_2(g) \quad (3)$$

since an significant amount of carbon remains in the material, any CO_2 produced will be consumed

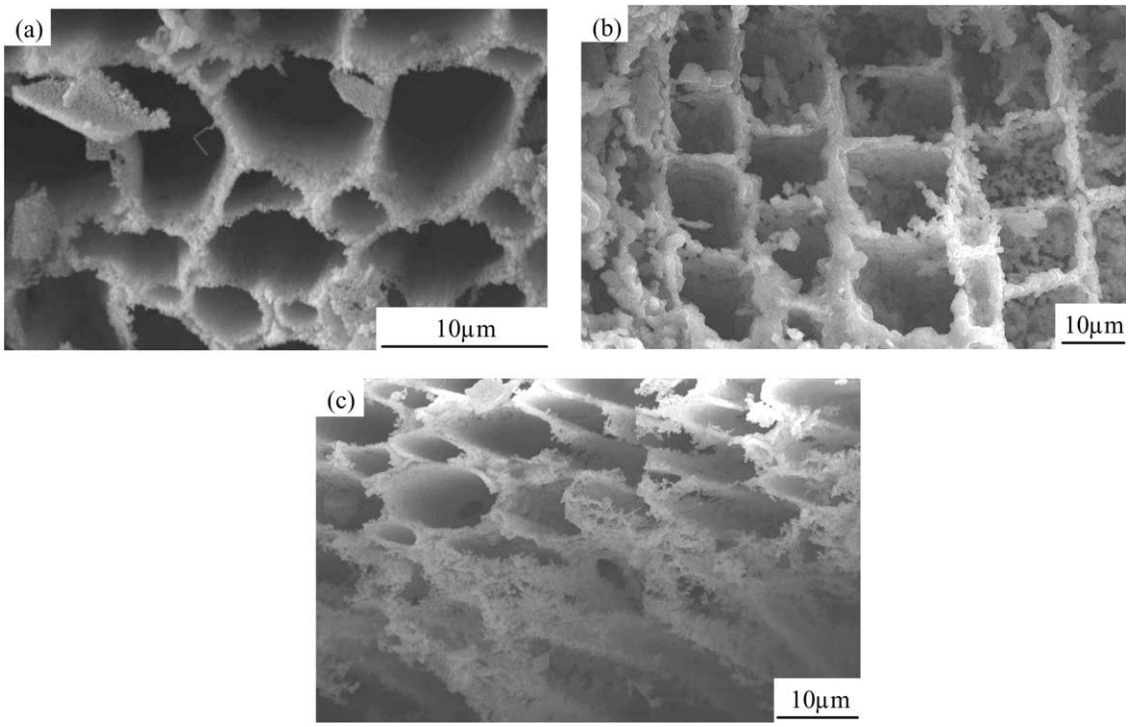

Fig. 9. SEM micrographs of woodlike SiC ceramics sintered at 1600 °C for 4 h, after impregnation procedure is repeated (a) 1, (b) 5 and (c) 9 times, respectively.

immediately by the Boudouard reaction (4) to form CO gas

$$CO_2(g) + C(s) \rightarrow 2CO(g) \quad (4)$$

In these reactions, carbon is either a CO_2 getter or a CO generator, which keeps the CO_2/CO ratio low enough to make the reduction of SiO_2 possible by gas phase CO.

In a second step, the gaseous silicon monoxide (SiO) subsequently reacts further with carbon according to the following gas-solid reaction:

$$SiO(g) + 2C(s) \rightarrow SiC(s) + CO(g) \quad (5)$$

The SiO vapor from Eqs. (2) and (3) reacts with carbon to yield SiC(s) nuclei heterogeneously on the surfaces of carbon through Eq. (5), which is commonly accepted mechanism of bulk SiC formation.[39] The synthesized SiC is strongly dependent of the carbon source,[40] which makes it possible that the resulting SiC ceramic is of a woodlike microstructure. In general, as soon as SiC forms on carbon, the growth process via Eq. (5) can be hindered by either the solid diffusion of carbon or the diffusion of SiO gas molecules through SiC layer. In the present work, the struts are porous after initial carbothermal reduction reaction (Fig. 9), which provides the paths for diffusion of SiO gas molecules into carbonaceous cell wall, allowing reaction (5) to continue.

Under SEM investigations, it is noted that there also exist whiskers (or fibers) of SiC in few cellular pores, which are randomly deposited as shown in Fig. 8d for an example. The formation of SiC whisker/fiber cannot be explained by the gas–solid reaction of SiO(g) and C(s). It is more likely that the whisker/fiber formed via gas-gas reaction between SiO(g) and CO(g) such that the morphology of the SiC could be totally independent of the morphology of carbon sources. The reaction can proceed as follows:[41]

$$SiO(g) + 3CO(g) \rightarrow SiC(s) + 2CO_2(g) \quad (6)$$

Reaction (6) favors the growth of SiC whiskers that are similar to those obtained by chemical vapor deposition with SiO and CO as the primary reactants in the literature.[18,42]

In our experiments, the carbothermal reduction was carried out in static argon atmosphere, thus the SiO gas pressure could be maintained much higher than when argon gas was flowing into the reaction chamber and carrying the SiO gas out of the furnace. Hence, under very high SiO partial pressure the disproportionation reaction of gaseous SiO into Si and SiO_2 can take place according to the reaction

$$2SiO(g) \rightarrow Si(s) + SiO_2(s) \quad (7)$$

The resulting Si would react with carbon to give rise to spherical SiC particles[43,44] according to the following reaction

$$Si(s) + C(s) \rightarrow SiC(s) \quad (8)$$

When the impregnation procedure was repeated many times, the obvious decrease of thickness and density of SiC struts was found, which may be due to its reaction with the remaining oxide since nearly all the carbon has been consumed:

$$SiC(s) + SiO_2(s) \rightarrow 3SiO(g) + CO(g) \quad (9)$$

Hence, a fraction of resulting SiO(g) and CO(g) escapes from the struts, which results in the increase in porosity of SiC struts, the decreasing of struts thickness and the formation of SiC whiskers in some places.

Therefore, both gas–solid and gas–gas reactions occurred during the preparation of porous SiC ceramic with a woodlike microstructure by a sol-gel method. However, it must be noted that the amount of whiskers is quite small in comparison to the amount of bulk SiC as confirmed by SEM, which indicates the gas–solid reaction is dominant.

4. Conclusions

Highly porous SiC ceramic with a woodlike microstructure was prepared at 1600 °C for 4 h in a static argon atmosphere by sol-gel and carbothermal reduction techniques using TEOS and tilia amurensis wood as the starting materials. The resulting SiC ceramic is composed of β-SiC with traces of α-SiC. The strut thickness of porous SiC ceramic becomes thinner with increasing the number of cycles of impregnation procedure. Five cycles of impregnation procedure, i.e., C-to-SiO_2 molar ratio≈3, is established as an optimum value for the preparation of porous biomorphic SiC ceramic. The free carbon content in porous SiC ceramic prepared using this procedure is controllable by the number of cycles of impregnation procedure. Bulk SiC struts and SiC whiskers in the resulting porous SiC ceramic are formed by gas–solid reaction of SiO(g) and C(s) and gas–gas reaction of SiO(g) and CO(g), respectively. Conversion of wood into ceramic materials with microstructures pseudomorphous to the bioorganic template anatomy offers a great potential for designing novel ceramics with anisotropic cellular morphologies.

Acknowledgements

This study was supported by the National Natural Science Foundation of China (No. 50272051 and No. 59872025).

References

1. Greil, P., Vogli, E., Fey, T., Bezold, A., Popovska, N., Gerhard, H. and Sieber, H., Effect of microstructure on the fracture behavior of biomorphous silicon carbide ceramics. *J. Eur. Ceram. Soc.*, 2002, **22**(14–15), 2697–2707.
2. Shin, D. W., Park, S. S., Choa, Y. H. and Niihara, K., Silicon/silicon carbide composites fabricated by infiltration of a silicon melt into charcoal. *J. Am. Ceram. Soc.*, 1999, **82**(11), 3251–3253.
3. Ota, T., Imaeda, M., Takase, H., Kobayashi, M., Kinoshita, N., Hirashita, T., Miyazaki, H. and Hikichi, Y., Porous titania ceramic prepared by mimicking silicified wood. *J. Am. Ceram. Soc.*, 2000, **83**(6), 1521–1523.
4. Singh, M. and Salem, J. A., Mechanical properties and microstructure of biomorphic silicon carbide ceramics fabricated from wood precursors. *J. Eur. Ceram. Soc.*, 2002, **22**(14–15), 2709–2717.
5. Gibson, L. J., Wood: a natural fibre reinforced composite. *Met. Mat.*, 1992, **8**, 333–338.
6. Greil, P., Lifka, T. and Kaindl, A., Biomorphic cellular silicon carbide ceramics from wood: I. processing and microstructure; II. mechanical properties. *J. Eur. Ceram. Soc.*, 1998, **18**(14), 1961–1975.
7. Hirose, T., Fan, T. X., Okabe, T. and Yoshimura, M., Effect of carbonizing speed on the property changes of woodceramics impregnated with liquefacient wood. *Mat. Lett.*, 2002, **52**(3), 229–233.
8. Xie, X. Q., Fan, T. X., Sun, B. H., Zhang, D., Sakata, T., Mori, H. and Okabe, T., Dry sliding friction and wear behavior of woodceramics/Al-Si composites. *Mat. Sci. Eng.*, 2003, **A342**(1–2), 287–293.
9. Muñoz, A., Martínez Fernández, J. and Singh, M., High temperature compressive mechanical behavior of joined biomorphic silicon carbide ceramics. *J. Eur. Ceram. Soc.*, 2002, **22**(14–15), 2727–2733.
10. Vogli, E., Sieber, H. and Greil, P., Biomorphic SiC-ceramic prepared by Si-vapor phase infiltration of wood. *J. Eur. Ceram. Soc.*, 2002, **22**(14–15), 2663–2668.
11. Sun, B. H., Fan, T. X. and Zhang, D., Porous TiC ceramics derived from wood template. *J. Porous Mat.*, 2002, **9**(4), 275–277.
12. Martínez-Fernández, J., Valera-Feria, F. M. and Singh, M., High temperature compressive mechanical behavior of biomorphic silicon carbide ceramics. *Scripta Mat.*, 2000, **43**(9), 813–818.
13. Qiao, G. J., Ma, R., Cai, N., Zhang, C. G. and Jin, Z. H., Mechanical properties and microstructure of Si/SiC materials derived from native wood. *Mat. Sci. Eng.*, 2002, **A323**(1–2), 301–305.
14. Qian, J. M., Wang, J. P., Jin, Z. H. and Qiao, G. J., Preparation of macroporous SiC from Si and wood powder using infiltration-reaction process. *Mat. Sci. Eng.*, 2003, **A358**(1–2), 304–309.
15. Vogli, E., Mukerji, J., Hofman, C., Kladny, R., Sieber, H. and Greil, P., Conversion of oak to cellular silicon carbide ceramic by gas-phase reaction with silicon monoxide. *J. Am. Ceram. Soc.*, 2001, **84**(6), 1236–1240.
16. Varela-Feria, F. M., Martínez-Fernández, J., de Arellano-López, A. R. and Singh, M., Low density biomorphic silicon carbide: microstructure and mechanical properties. *J. Eur. Ceram. Soc.*, 2002, **22**(14–15), 2719–2725.
17. Ota, T., Takahashi, M., Hibi, T., Ozawa, M., Suzuki, S., Hikichi, Y. and Suzuki, H., Biomimetic process for producing SiC wood. *J. Am. Ceram. Soc.*, 1995, **78**(12), 3409–3411.
18. Vix-Guterl, C., McEnaney, B. and Ehrburger, P., SiC material produced by carbothermal reduction of a freeze gel silica-carbon artefact. *J. Eur. Ceram. Soc.*, 1999, **19**(4), 427–432.
19. Koc, R., Glatzmaier, G. and Sibold, J., β-SiC production by reacting silica gel with hydrocarbon gas. *J. Mat. Sci.*, 2001, **36**(4), 995–999.
20. Meng, G. W., Cui, Z., Zhang, L. D. and Phillipp, F., Growth and characterization of nanostructured β-SiC via carbothermal reduction of SiO_2 xerogels containing carbon nanoparticles. *J. Cryst. Growth*, 2000, **209**(4), 801–806.

21. Hasegawa, I., Nakamura, T., Motojima, S. and Kajiwara, M., Synthesis of silicon carbide fibers by sol-gel processing. *J. Sol-gel Sci. Technol*., 1997, **8**(1–3), 577–579.
22. Real, C., Alcalá, D. and Criado, J. M., Synthesis of silicon carbide whiskers from carbothermal reduction of silica gel by means of the constant rate thermal analysis (CRTA) method. *Solid State Ionics*, 1997, **95**(1–2), 29–32.
23. Li, J. W., Tian, J. M. and Dong, L. M., Synthesis of SiC precursors by a two-step sol-gel process and their conversion to SiC powders. *J. Eur. Ceram. Soc*., 2000, **20**(11), 1853–1857.
24. Hasegawa, I., Nakamura, T., Motojima, S. and Kajiwara, M., Silica gel-phenolic resin hybrid fibres: new precursors for continuous beta-silicon carbide fibres. *J. Mat. Chem*., 1995, **5**(1), 193–194.
25. Li, X. K., Liu, L., Zhang, Y. X., Shen, S. D., Ge, S. and Ling, L. C., Synthesis of nanometre silicon carbide whiskers from binary carbonaceous silica aerogels. *Carbon*, 2001, **39**(2), 159–165.
26. Vix-Guterl, C. and Ehrburger, P., Effect of the properties of a carbon substrate on its reaction with silica for silicon carbide formation. *Carbon*, 1997, **35**(10–11), 1587–1592.
27. Vix-Guterl, C., Alix, I., Gibot, P. and Ehrburger, P., Formation of tubular silicon carbide from a carbon-silica material by using a reactive replica technique: infra-red characterization. *Appl. Surf. Sci*., 2003, **210**(3–4), 329–337.
28. Jin, G. Q. and Guo, X. Y., Synthesis and characterization of mesoporous silicon carbide. *Micropor. Mesopor. Mat*., 2003, **60**(1–3), 207–212.
29. Preiss, H., Berger, L. M. and Braun, M., Formation of black glasses and silicon carbide from binary carbonaceous/silica hydrogels. *Carbon*, 1995, **33**(12), 1739–1746.
30. Greil, P., Biomorphous ceramics from lignocellulosics. *J. Eur. Ceram. Soc*., 2001, **21**(2), 105–118.
31. Ehrburger, P., Lahaye, L. and Wozniak, E., Effect of carbonization on the porosity of beechwood. *Carbon*, 1982, **20**(5), 433–439.
32. Byrne, C. E. and Nagle, D. C., Carbonization of wood for advanced materials applications. *Carbon*, 1997, **35**(2), 259–266.
33. Frevel, L. K., Petersen, D. R. and Saha, C. K., Polytype distribution in silicon carbide. *J. Mat. Sci*., 1992, **27**(7), 1913–1925.
34. Baraton, M. I. and El-shall, M. S., Synthesis and characterization of nanoscale metal oxides and carbides: II. micro-Raman and FT-IR surface studies of a silicon carbide powder. *Nanostruct. Mat*., 1995, **6**(1–4), 301–304.
35. Kirchschstein, G., *Gmelin Handbook of Inorganic Chemistry, Si-Silicon Supplement, 8th ed., vol. B2*. Springer, Berlin, 1984.
36. Paccaud, O. and Derré, A., Silicon carbide coating by reactive pack cementation—part I: silicon carbide/silica interaction. *Chem. Vapor Depos*., 2000, **6**(1), 33–40.
37. Paccaud, O. and Derré, A., Silicon carbide coating by reactive pack cementation—part II: silicon monoxide/carbide reaction. *Chem. Vapor Depos*., 2000, **6**(1), 41–50.
38. Holmberg, S., Persson, K. and Peterson, H., Nonlinear mechanical behaviour and analysis of wood and fibre materials. *Comput. Struct*., 1999, **72**(4–5), 459–480.
39. Martin, H. P., Ecke, R. and Müller, E., Synthesis of nanocrystalline silicon carbide powder by carbothermal reduction. *J. Eur. Ceram. Soc*., 1998, **18**(12), 1737–1742.
40. Lin, Y. J. and Tsang, C. P., The effects of starting precursors on the carbothermal synthesis of SiC powders. *Ceram. Int*., 2003, **29**(1), 69–75.
41. Koc, R. and Cattamanchi, S. V., Synthesis of beta silicon carbide powders using carbon coated fumed silica. *J. Mat. Sci*., 1998, **33**(10), 2537–2549.
42. Saito, M., Nagashima, S. and Kato, A., Crystal growth of SiC whisker from the SiO(g)–CO system. *J. Mat. Sci. Lett*., 1992, **11**(7), 373–376.
43. Krstic, V. D., Production of fine, high-purity beta silicon carbide powders. *J. Am. Ceram. Soc*., 1992, **75**(1), 170–174.
44. Seo, W. S. and Koumoto, K., Stacking faults in β-SiC formed during carbothermal reduction of SiO_2. *J. Am. Ceram. Soc*., 1996, **79**(7), 1777–1782.